Supporting Information

Flexible and Reusable Piezo-responsive Ternary Bionanocomposite Membrane for Energy Generation and Catalytic Removal of Organic Pollutants

Indrajit Mondal[a], Piyali Halder[a], Somen Biswas[a, b], Souvik Sau[a, b], Saheli Ghosh[a], Shireen Sultana [a], Rajat Kanti Chatterjee [c], Dheeraj Mondal*[d], Pabitra Kumar Paul*[a], Sukhen Das*[a]

[a] Department of Physics, Jadavpur University, Kolkata-700032, India.

[b] Department of Physics, Bangabasi College, Kolkata-700009, India.

[c] Department of Physics, West Bengal State University, Berunanpukhuria, West Bengal-700126, India

[d] Department of Physics, Nabagram Hiralal Paul College, Hooghly-712246, India.

[*]Address for Correspondence

sdasphysics@gmail.com

pabitrak.pal@jadavpuruniversity.in

dheerajphysics92@gmail.com

S1. Experimental Section

S1.1. Materials

All reagents utilized in this study were of analytical grade to ensure high experimental fidelity. 2′,7′-Dichlorodihydrofluorescein diacetate (DCFDA, $\geq$ 97% purity, 10 μM), chitosan (purity 99.99%, molecular weight: 190,000–310,000 Da), tert-butyl acrylate (TBA), p-benzoquinone (p-BQ), silver nitrate ($AgNO_3$), Congo Red (CR), Methylene Blue (MB), Methyl Orange (MO), and ethylenediaminetetraacetic acid disodium salt (EDTA) were procured from Sigma-Aldrich and used without further purification. For microbiological assessments, phosphate-buffered saline (PBS), absolute ethanol (99%), and Luria–Bertani (LB) medium were procured from Hi

Media Pvt. Ltd., India. The clinical strain *Enterococcus faecalis* (*E. faecalis*), a known skin-pathogenic Gram-positive bacterium, was obtained from the Microbial Type Culture Collection (MTCC) at IMTECH, Chandigarh, India. Deionized water with a resistivity of 18.2 $M\Omega \cdot cm$ and neutral pH, produced using a NW-Ultrapure Water System, was used consistently for all experimental procedures to ensure high purity.

S1.2. Synthesis of CMO decorated MCCNFs nanocomposite

Carbon nanofibers (MCCNFs) were synthesized from banana stem waste via a sintering-free chemical route[1]. The fibers were pre-soaked in Millipore water for 12 hours, sun-dried, chopped, and ultrasonically cleaned. Following overnight treatment with 10% KOH and neutralization, they were dried at $60^{\circ}C$. Oxidative functionalization was performed using a pre-chilled H_2SO_4: HNO_3 mixture (1:3:9), followed by the addition of $KClO_3$ (3:1, w/w) and stirring at $80^{\circ}C$ overnight. The resulting black fibers were thoroughly washed to neutral pH, dried at $80^{\circ}C$, and designated as MCCNFs. $CoMnO_3$ nanoparticles were synthesized via a modified wet chemical method using cobalt and manganese acetates with PVA as a capping agent[2]. The pH was adjusted to 10 using KOH, followed by overnight stirring, settling, washing, and drying at $80\ ^{\circ}C$. The dried product was sintered at $500^{\circ}C$ under vacuum for 4 hours, yielding phase-pure nanocrystals (CMO) with controlled crystallinity and minimal oxygen vacancies via an eco-friendly, cost-effective route. For the synthesis of the nanocomposite, MCCNFs and CMO were mixed in an equimolar ratio using a water–ethanol solvent system. The dispersion was mechanically stirred at 700 rpm for 2 hours, followed by ultrasonication at room temperature for 1 hour to promote uniform interaction. Post-treatment, the suspension was centrifuged, redispersed in ethanol, and dried at $70^{\circ}C$ overnight to obtain the final hybrid material for further analysis.

S1.3. Synthesis of chitosan-based bio-polymeric membrane

Chitosan-based membranes were prepared by dissolving 2 g of chitosan in 200 mL of 1% acetic acid under continuous stirring (500 rpm, 60 min), followed by dropwise NaOH addition to raise the pH to 10, inducing gelation. For the CHS-CMO composite, a pre-dispersed $CoMnO_3$ nanoparticle suspension was incorporated into the chitosan matrix prior to pH adjustment. In the CHS-MCCNFs/CMO hybrid, $CoMnO_3$ decorated chemically derived carbon nanofibers (MCCNFs) were co-integrated into the chitosan solution. The resulting mixtures were cast onto petri dishes and dried at 50 ℃ to yield uniform, flexible, and self-standing membranes. The synthesis process is detailed in **Figure S1.** All samples were systematically characterized and employed for comparative functional analyses.

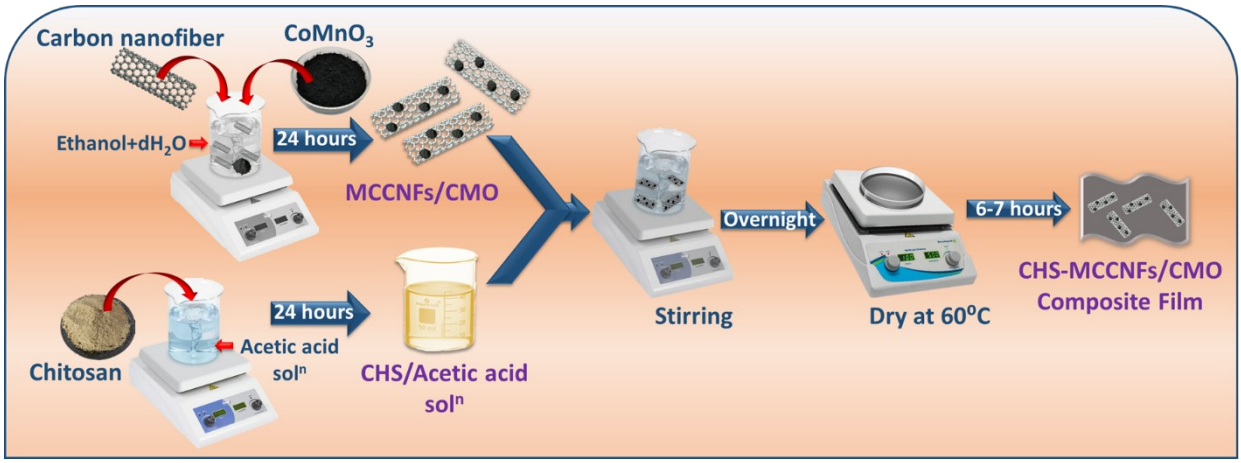

Figure S1: A schematic illustration of chitosan-based ternary bio-nanocomposite membrane using a cost-effective solution-casting technique

S1.4. Characterization Techniques

Structural and phase analysis was performed using X-ray diffraction (Bruker AXS D8), confirming high crystallinity and purity. Phonon vibrations in MCCNFs/CMO were examined via Raman spectroscopy (Newport RS 2000™) to assess lattice dynamics while nanoscale features were visualized using HR-TEM (JEOL JEM-2100 Plus). Functional groups and vibrational modes were identified via FTIR (PerkinElmer Spectrum 100). Surface morphology

and elemental distribution were characterized by FESEM (ZEISS GeminiSEM 450) with EDX

Surface charge (zeta potential, Malvern Zetasizer) and frequency-dependent dielectric parameters were evaluated using an LCR meter (HP 4274A) across 40 Hz-1MHz at room temperature. Ferroelectric properties were evaluated through P–E loop measurements (Precision Premier II, Radiant Technologies). Thermal stability was assessed via TGA–DTA (Shimadzu DTA-60H). UV–vis absorption spectra were recorded using a Lambda 365 spectrophotometer. Dye mineralization was quantified by TOC analysis (Shimadzu TOC-VCPH), and ROS generation during stimuli antibacterial testing was assessed using a Cary Eclipse fluorescence spectrophotometer (Agilent Technologies).

S1.5. Piezo-catalytic carcinogenic dye degradation

S1.5.1. Dye Degradation Experimental Setup

Congo Red (CR) dye solutions were prepared in distilled (DI) water at concentrations of 2.5, 5, and 10 ppm, while Methylene Blue (MB), Methyl Orange (MO), and a CR–MB mixed dye (1:1) were prepared at 2.5 ppm. A 1 cm $\times$ 1 cm CHS-MCCNFs-CMO membrane was immersed in 200 mL of each dye solution in separate glass vials. To evaluate comparative performance, CHS and CHS-CMO membranes were also tested under identical conditions. Prior to sonication, membranes were soaked in the dye solutions under dark conditions for 30 minutes to attain adsorption–desorption equilibrium (ADE). Ultrasonication was carried out using a Telsonic ultrasonic bath (33 W, 15 $\pm$ 5 kHz). To monitor degradation, 3 mL aliquots were extracted every 5 minutes and returned post-analysis, maintaining a constant 200 mL volume. To minimize thermal degradation and solvent loss from ultrasonic heating, bath water was replaced every 10 minutes, ensuring consistent reaction conditions.

S1.5.2. Reactive Species Scavenger's Experiments

Scavenger studies were performed to identify reactive species responsible for degradation. In separate 200 mL CR solutions (2.5 ppm), 1 cm × 1 cm CHS-MCCNFs-CMO membranes were treated with 0.5 mM scavengers: EDTA (holes, h^+), p-benzoquinone (superoxide radicals, $\cdot O_2^-$), $AgNO_3$ (electrons, e^-), and DMSO (hydroxyl radicals, ·OH). Ultrasonication followed, and UV–vis spectra were recorded to analyze scavenger effects while maintaining a controlled temperature.

S1.5.3. ·OH Radical Confirmation via TA Fluorescence Probe

To verify hydroxyl radical generation, a 0.5 mM terephthalic acid (TA) solution was added to 200 mL of 2.5 ppm CR solution. After 35 minutes of ultrasonication, 3 mL aliquots were collected every 5 minutes for PL analysis at 315 nm excitation. A characteristic emission at 425 nm confirmed the formation of fluorescent 2-hydroxyterephthalic acid, indicating ·OH generation.

S1.5.4. Membrane Reusability

Post-reaction, membranes were rinsed with DI water, air-dried at 50℃ overnight, and inspected for damage. Only intact membranes were reused in subsequent cycles, ensuring experimental consistency and catalyst durability.

S1.6. Piezo-catalytic pharmaceutical degradation

To assess the piezocatalytic degradation capabilities of the films under study, experiments were carried out using two model antibiotics: tetracycline and ciprofloxacin. The tetracycline solution was prepared at a concentration of 0.2 mM, while the ciprofloxacin solution was created by diluting 0.1 mL of eye drops (containing 0.3% w/v ciprofloxacin and 0.01% w/v benzalkonium chloride) in 200 mL of distilled water. Prior to the piezocatalytic tests, both solutions underwent 60 minutes of sonication to achieve a uniform suspension. Each

piezocatalytic experiment utilized 100 mL of the prepared solution. Concentrations of the antibiotics were measured using a UV-visible spectrophotometer, with tetracycline and ciprofloxacin displaying absorption peaks around 357 nm and 277 nm, respectively. All other experimental parameters, such as sample size, ultrasonication conditions, and concentration measurements, were identical to those used in the piezocatalytic dye degradation experiments.

S1.7. Piezo-catalytic bacterial disinfection

S1.7.1. Experimental Design and Bacterial Viability Assessment

The study focused on examining the disinfection of gram-positive coliform bacteria, *E. faecalis*, through the process of piezocatalysis. To commence the experiment, sterile Luria–Bertani (LB) broth was inoculated with a 0.5 McFarland standard bacterial suspension and incubated overnight at 37℃ with continuous shaking at 120 rpm. The aim was to assess the effectiveness of the CHS-MCCNFs/CMO membrane in piezodynamic inactivation. Three sterile glass vials were prepared, and the inoculated solutions were divided into three parts, with two vials each containing 1 cm × 1 cm rectangular CHS-MCCNFs/CMO films. The control group, designated as group A, consisted of vials without any films or ultrasonic exposure. The remaining two vials were organized into groups B and C. Group B included only the bacterial cultures, which were subjected to 20 minutes of ultrasonic vibration. Group C consisted of both bacterial cultures and CHS-MCCNFs/CMO films, also exposed to ultrasonic treatment. Comparative piezocatalytic disinfection studies were conducted using CHS, and CHS-CMO. At regular 20-minute intervals, a 1 mL aliquot was taken from each experimental section. Each aliquot was diluted 1000-fold with sterile LB broth and then spread onto solid LB agar plates. The plates were incubated at 37℃ for 24 hours to allow for colony formation, enabling accurate counting. Each sample was analyzed in triplicate to ensure precision.

Bacterial mortality percentages were calculated using standard formulas based on colony counts.

S1.7.2. Reactive Oxygen Species (ROS) Quantification

This research also utilized piezocatalytic disinfection to harness reactive oxygen species (ROS) for bacterial inhibition. The amount of ROS generated in each sample was measured using 2',7'-dichlorofluorescein diacetate (DCFH-DA), which is effective for detecting a wide range of ROS. In the experimental procedure, 2 mL aliquots were collected and centrifuged at 4500 rpm for 6 minutes with a PBS solution for washing. After this, a 10 μM DCFH-DA solution was added. The samples were then incubated in the dark at 37°C for 30 minutes. Fluorescence intensity was subsequently assessed using a Fluorescence Spectrophotometer (Horiba-Fluromax-4C, USA), with excitation at 485 nm and emission at 520 nm. Upon interaction with ROS, DCFH-DA was converted into 2',7'-dichlorofluorescein (DCF), resulting in increased fluorescence that indicated ROS production.

S1.7.3. Morphological Analysis via FESEM

FESEM analysis was utilized to assess the damage caused to bacterial cells after treatment with CHS-MCCNFs/CMO combined with ultrasound. For sample preparation, both treated and control bacterial cells underwent an 18-hour incubation at 37°C. Following this, 1 mL of the incubated cultures-both control and treated-was centrifuged for 5 minutes at 4500 rpm to collect the precipitates. The precipitates from each vial were then washed with sterile, filtered PBS solution at 3000 rpm for 3 minutes. The resulting pellets were mixed with a 2% glutaraldehyde solution and subsequently diluted with ethanol at varying concentrations (5-100%). These mixtures were drop-cast onto clean coverslips and allowed to dry in a laminar airflow cabinet. FESEM analysis was carried out after gold coating and mounting the samples on carbon tape.

S1.7.4. Membrane Reusability Evaluation

Additionally, to evaluate the reusability of the membrane, this procedure was repeated four more times with the same membrane, providing a thorough assessment of its efficiency across multiple usage cycles.

S1.8. Hemolysis assay

The biocompatibility of the nanocomposite membranes was assessed through an *in vitro* hemolysis assay adapted from established protocols. Red blood cells (RBCs) were isolated from freshly collected Sprague-Dawley rat blood and purified using sterile phosphate-buffered saline (PBS). These RBCs were then incubated with dispersions of the CHS-MCCNFs/CMO nanocomposite. PBS-treated RBCs served as the negative control, while those exposed to ultrapure water acted as the positive control. Following incubation at $37^{\circ}C$ for one hour, samples were centrifuged at 3500 rpm for four minutes, and the absorbance of the supernatant was measured at 540 nm. The hemolysis percentage was calculated using the formula:

$$\text{Hemolysis rate} = \frac{A_{sample} - A_{negative\ control}}{A_{positive\ control} - A_{negative\ control}} \times 100\% \quad \text{(S1)}$$

The CHS-MCCNFs/CMO nanocomposite exhibited a pronounced ability to minimize RBC membrane disruption, effectively preventing hemolysis. This indicates that the material is non-cytotoxic to erythrocytes, thereby avoiding adverse effects such as excessive bleeding, inflammation, or delayed wound repair. In contrast, complete hemolysis was observed in the ultrapure water control, evident from the characteristic red coloration of the solution due to total RBC lysis.

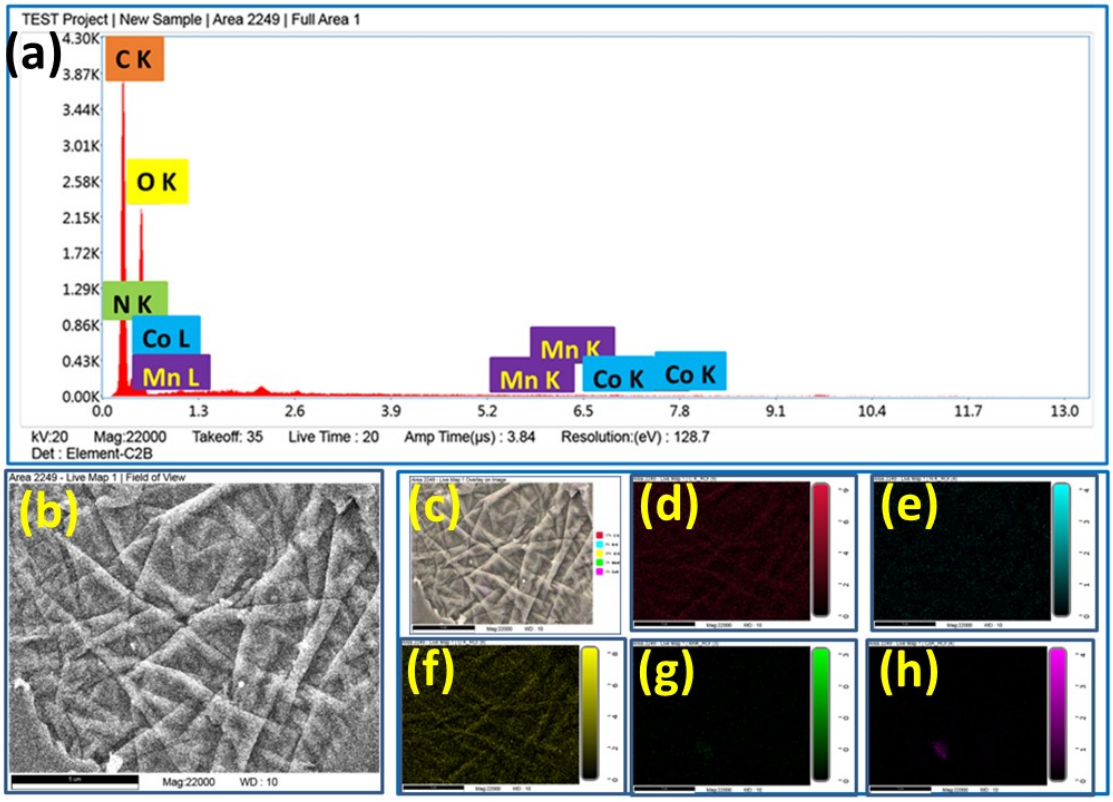

Figure S2: (a) EDX spectra and (b-h) elemental mapping analysis of CHS-MCCNFs/CMO ternary bio-nanocomposite membrane.

S2. Device Fabrication

Among all membranes, CHS-MCCNFs/CMO exhibited the highest piezoelectric response and was thus chosen for energy harvesting applications. A 1 cm × 1 cm membrane was integrated with aluminium electrodes connected via copper wires on both sides, forming the device shown in **Figure 4(c-d)**. To ensure mechanical stability and protection, the assembly was encapsulated in a PET-coated jacket.

S3. Force Calculation

The force (F) was determined using the equation to:

$$F = m\left(\frac{v}{\Delta t} + g\right) \tag{S2}$$

Where, all parameters have their own physical meanings. The velocity was derived from the equation,

$$mgh = \frac{1}{2}mv^2 \tag{S3}$$

Table S1

Comparative summary of the piezoelectric coefficient and dielectric constants of various nanocomposite membranes reported in literature (N.R.=Not reported).

Sample Name	Synthesis method	Dielectric Constant	Piezoelectric coefficient (d_{33} pC/N)	References
Collagen-chitosan	Solution casting	N.M.	0.212	[3]
Glycine/Chitosan	Drop casting	7.7	N.M.	[4]
Chitosan+ 15 wt% POZ	Solution casting	6.48	N.R.	[5]
CS/hydroxylated $BaTiO_3$	Solvent casting	N.R.	11.29	[6]
Chitosan 60F	Solvent casting	N.R.	15.56	[7]
Chitosan	N.R.	N.R.	18.4	[8]
Chitosan/PVDF	Electrospinning	8	35	[9]
CHS-MCCNFs/CMO	Solution casting	86	62.14	**This work**

Table S2

A comparative analysis of the piezoelectric voltage, current, and power density of all three samples.

SL No.	Sample Id	Voltage (V)	Current (μA)	Power density (mW cm^{-3})
1	**CHS**	**1.37**	**11.9**	**0.709**
2	**CHS-CMO**	**6.1**	**17.9**	**4.748**
3	**CHS-MCCNFs/CMO**	**10.15**	**22.4**	**9.885**

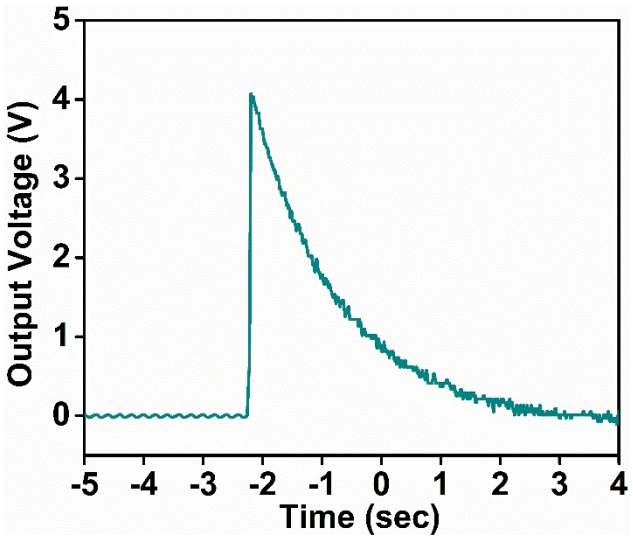

Figure S3: Discharge profile of the 1 μF capacitor charged up to 4 V with 60 s of finger tapping.

Table S3

A comparative analysis of the piezoelectric voltage generation using the ternary bio-nanocomposite membranes in contrast to other reported studies (N.R.=Not reported).

Sample Name	**Type of Composite**	**Place/ Motion**	**Piezoelectric Voltage**	**Current**	**Power density**	**References**
Graphene (0.03 wt%) PVDF-TrFE-nanobelts	Synthetic	N.R.	35 mV	N.R.	N.R.	[10]
Au/ZnO	Synthetic	Electro-stimulation	140 mV	N.R.	1.5 W/cm^2	[11]
AIN	Synthetic	Finger Bending	0.7 V	N.R.	0.4 mW/ cm^3	[12]
PLLA	Synthetic	External Force	1 V	30-400 nA	0.07 μW/cm^2	[13]
MoS_2 shell array	Synthetic	Under a pressure of 4.2 kPa	1.2 V	N.R.	8.07 μW/m^2	[14]
P(VDF-TrFE)	Synthetic	N.R.	1.7 V	41.5 nA	N.R.	[15]
SiO_2/ZnO	Synthetic	Foot Press	2.5 V	N.R.	N.R.	[16]
MnO_2/PVDF	Synthetic	Hammer Tapping	3.2 V	N.R.	N.R.	[17]

ZnO-nanorod	Synthetic	Palm Clapping	5V	N.R.	40-80 nW	[18]
CHS-MCCNFs/ CMO	**Biopolymer**	**Finger Tapping, Water flow**	**10.15 V, 3.1 V**	**22.4 μA**	**9.885 mW c m^{-3}**	**This work**

Table S4

Comparative assessment of carcinogenic dye degradation efficiency of ternary bio-nanocomposite membranes against previously reported piezocatalytic systems.

SL NO.	Sample Name	Types of Polymers	Degradation Efficiency (%)	Target Effluent	Degradation Time (mins)	Types of Vibration	References
1	MoS_2 nano flower/PVDF	Synthetic	> 90	Rhodamine-B	20	Ultrasonic vibration	[19]
2	TiO_2/PVDF	Synthetic	100	Methylene blue	40	Ultrasonic vibration	[20]
3	PVDF/$ZnSnO_3$-Co_3O_4	Synthetic	100	Methylene blue, rhodamine-B	20	Ultrasonic vibration	[21]
4	PDMS/WS_2 nanoflower	Synthetic	99	Rhodamine-B	90	Ultrasonic vibration	[22]
5	PDMS/MoS_2	Synthetic	67	Rhodamine-B	200	Ultrasonic vibration	[23]
6	$BaTiO_3$/PDMS	Synthetic	94	Rhodamine-B	120	Ultrasonic vibration	[24]
7	PTFE	Synthetic	89.7 (MO), > 90 (MB, AO7)	Methyl orange, acid orange-7, methylene blue	60	Ultrasonic vibration	[25]
8	Fe0 /PANI	Synthetic	98	Congo red	30	Ultrasonic vibration	[26]
9	Chitosan modified montmorillonite	Biopolymer	82.74	Acid orange-7, basic red, basic yellow	60	Ultrasonic vibration	[27]
10	**CHS-MCCNFs/CMO**	**Biopolymer**	**99.27**	**Congo red**	**35**	**Ultrasound**	**This Work**

Table S5

Post CR dye degradation phytotoxicity evaluation

Parameters	Control (Distilled Water)	CR Dye-contained Water	Degraded Dye Water
Germination (%)	100.00	63.7	89.65

Plant fresh weight (g)	1.123	0.6532	0.9987
Plant dry weight (g)	0.2232	0.0789	0.1876
Average Plant height (cm)	11.6	6.3	9.9

Table S6

Assessment of water quality parameters pre- and post-catalysis in different water types

Condition	**Distilled Water (D.I.)**			**Wastewater**			**Drinking Water**		
	pH	TDS (ppm)	Conductivity ($\mu S/cm$)	pH	TDS (ppm)	Conductivity ($\mu S/cm$)	pH	TDS (ppm)	Conductivity ($\mu S/cm$)
Before catalysis	6.32	5.0	9.0	6.57	1201.0	2415.0	6.99	237.0	309.0
Dye control (no catalyst)	6.89	8.0	13.0	6.72	1219.0	2482.0	7.29	269.0	316.0
Dye + Catalyst (Before reaction)	6.89	11.0	19.0	6.92	1327.0	2444.0	7.17	297.0	323.0
Post-catalysis (Before extraction)	7.11	7.0	12.0	7.19	1199.0	2099.0	7.42	231.0	337.0
Post-catalysis (After extraction)	6.89	6.0	6.0	6.59	1198.0	2379.0	7.08	177.0	321.0

Table S7

Comparative Study on Pharmaceutical Degradation using CHS-MCCNFs/CMO and other reported piezocatalysts.

Sample Name	**Form of piezocatalyst**	**Pharmaceutical**	**Sonicator Specification**	**Degradation time (min)**	**Degradation efficiency (%)**	**References**
Ag@$LiNbO_3$/PVDF	film	tetracycline, ciprofloxacin	40 kHz, 120 W	120	69,53	[28]
$Ba_{0.85}Ca_{0.15}Ti_{0.9}Zr_{0.1}O_3$	powder	ciprofloxacin	40 kHz, 70 W	180	70	[29]
30 wt% $BaTiO_3$/cement	pellet	paracetamol	40 kHz, 70 W	240	70	[30]
$Ba_{0.9}Ca_{0.1}Ce_xTi_{1-x}O_3$ (x=0.15)	powder	ibuprofen	40 kHz, 110 W	120	75	[31]
$BaTiO_3$	powder	ciprofloxacin	40 kHz, 70 W	150	85	[32]

CHS-MCCNFs/CMO	**Bio-nanocomposite membrane**	**ciprofloxacin, tetracycline**	**15 kHz, 33 W**	**60**	**97.9, 90.8**	**This work**

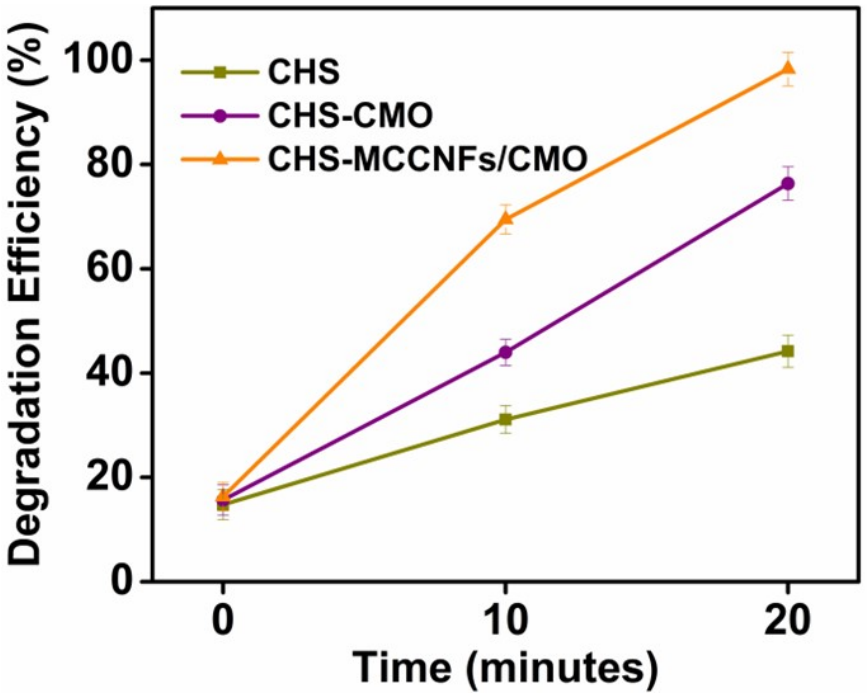

Figure S4: A comparative bacterial mortality data from the agar plate counting using different samples

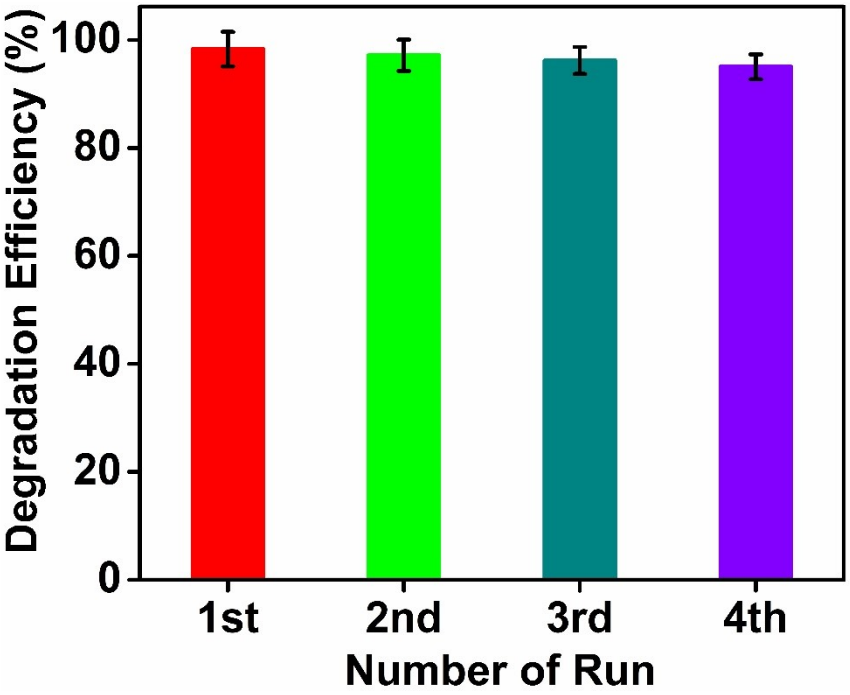

Figure S5: Recyclability test of the CHS-MCCNFs/CMO membrane for *E. faecalis* bacteria

Table S8

A comparative analysis of the piezocatalytic coliform *E. faecalis* bacterial eradication using the ternary bio-nanocomposite membranes in contrast to other reported studies.

SL NO.	Sample Name	Form of Piezocatalyst	Synthesis Process	Degradation Efficiency (%)	Degradation Time (mins)	Types of Vibration	Reference
1	$CoMnO_3$	Powder	Modified Chemical Method	95%	60	Ultrasonic vibration	[2]
2	$BaTiO_3$	Powder	Hydrothermal Method	99%	30	Soft Ultrasound	[33]
3	ZnO/CHS	Hydrogel	In situ chemical precipitation	96%	20	Ultrasonic vibration	[34]
4	kaolinite clay-doped (PVDF-HFP)	Synthetic Polymer	Solution-Casting	97%	40	Ultrasonic vibration	[35]
5	BF@PV5	Synthetic	Solution-Casting	99.9%	30	Ultrasonic vibration	[36]
6	ZO@CHS	Biopolymer	Solution-	97.21%	20	Ultrasonic	[37]

			Casting			vibration	
7	**CHS-MCCNFs/CMO**	**Biopolymer**	**Solution-Casting**	**98.31%**	**20**	**Soft Ultrasound**	**This Paper**

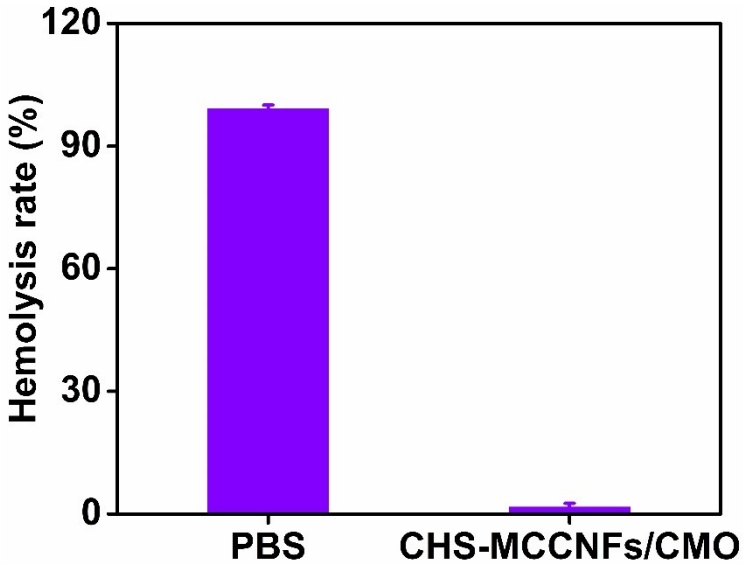

Figure S6: Biocompatibility of the CHS-MCCNFs/CMO by Hemolysis rate technique

References

1 I. Mondal, P. Halder, M. Kundu, B. K. Paul, S. Biswas, A. Pal, S. Sau, D. Mondal, P. K. Paul and S. Das, *Mater. Today Chem.*, 2024, **35**, 101905.

2 I. Mondal, P. Halder, A. Chatterjee, N. Bag and S. Sau, *J. Environ. Chem. Eng.*, 2024, **12**, 112385.

3 S. D. Figueiro, A. S. B. Sombra, C. C. Silva, C. G. A. Lima, A. G. Pinheiro and J. C. Go, 2001, 1–4.

4 E. S. Hosseini, L. Manjakkal, D. Shakthivel and R. Dahiya, , DOI:10.1021/acsami.9b21052.

5 S. B. Aziz, M. H. Hamsan, M. F. Z. Kadir and H. J. Woo, , DOI:10.1155/2020/8586136.

6 E. Prokhorov, G. L. Bárcenas, B. Liliana, E. Sánchez, B. Franco, F. Padilla-vaca, M. Adelaido, H. Landaverde, J. Martín and Y. Limón, *Colloids Surfaces B Biointerfaces*, 2020, **196**, 111296.

7 G. De Marzo, V. M. Mastronardi, L. Algieri, F. Vergari, F. Pisano, L. Fachechi, S. Marras, L. Natta, B. Spagnolo, V. Brunetti, F. Rizzi, F. Pisanello and M. De Vittorio, , DOI:10.1002/aelm.202200069.

8 E. Praveen, S. Murugan and K. Jayakumar, 2017, 35490–35495.

9 C. Hung, Y. Lin and T. Y. Ã, 2006, **27**, 4461–4469.

10 Y. Han, C. Jiang, H. Lin, C. Luo, R. Qi and H. Peng, 2020, **1901249**, 1–8.

11 K. Ma, G. Qi, B. Wang, T. Yu, Y. Zhang, H. Li, S. Addisu and Y. Jin, *Nano Energy*, 2021, **87**, 106208.

12 F. Guido, A. Qualtieri, L. Algieri, E. Domenico, M. De Vittorio and M. Teresa, *MEE*, 2016, **159**, 174–178.

13 M. J. Higgins, .

14 J. Kyu, S. Kim, S. Jang, Y. Rang, S. Kim, H. Chang, W. Song, S. Sook, J. Lim, K. An and S. Myung, *Nano Energy*, 2019, **61**, 471–477.

15 A. Wang, M. Hu, L. Zhou and X. Qiang, 2019, 1–16.

16 S. Panda, S. Hajra, K. Mistewicz, P. In-na, M. Sahu, P. M. Rajaitha and H. Joon, *Nano Energy*, 2022, **100**, 107514.

17 Q. Zhao, L. Yang, K. Chen, Y. Ma, Q. Peng, H. Ji and J. Qiu, *Compos. Sci. Technol.*, 2020, **199**, 108330.

18 Z. Zhang, Y. Chen and J. Guo, *Phys. E Low-dimensional Syst. Nanostructures*, 2019,

105, 212–218.

19 B. Bagchi, N. Amin, N. Janowicz, S. Das and K. Tiwari, *Nano Energy*, 2020, **78**, 105339.

20 C. Dong, Y. Fu, W. Zang, H. He, L. Xing and X. Xue, *Appl. Surf. Sci.*, 2017, **416**, 424–431.

21 T. D. Raju, S. Veeralingam and S. Badhulika, , DOI:10.1021/acsanm.0c00771.

22 S. Masimukku, Y. Hu, Z. Lin, S. Chan and T. Chou, *Nano Energy*, 2018, **46**, 338–346.

23 J. Lin, Y. Tsao, M. Wu, T. Chou and Z. Lin, *Nano Energy*, 2017, **31**, 575–581.

24 W. Qian, K. Zhao, D. Zhang, C. R. Bowen, Y. Wang and Y. Yang, , DOI:10.1021/acsami.9b07857.

25 Y. Wang, Y. Xu, S. Dong, P. Wang, W. Chen, Z. Lu, B. Pan, D. Wu, C. D. Vecitis and G. Gao, 2021, 1–8.

26 R. Das, M. Bhaumik, S. Giri and A. Maity, *Ultrason. - Sonochemistry*, 2017, 0–45.

27 S. Karaca, E. Ç. Onal, O. Açıs and A. Khataee, , DOI:10.1016/j.matchemphys.2020.124125.

28 G. Singh, M. Sharma and R. Vaish, , DOI:10.1021/acsami.1c01314.

29 J. A. Phys, 2020, **135103**, 0–10.

30 M. Sharma, A. Chauhan and R. Vaish, *Mater. Res. Bull.*, 2021, **137**, 111205.

31 M. Sharma, A. Halder and R. Vaish, 2020, **122**, 1–8.

32 J. Xu, T. Zang and R. Vaish, 2021, 1661–1668.

33 N. Bag, J. Roy, D. Mondal, S. Ghosh, S. Bardhan, S. Roy, S. Bhandary and S. Das,

Ceram. Int., , DOI:10.1016/j.ceramint.2023.12.128.

34 A. Banerjee, A. Mukherjee, N. Bag, P. Halder, I. Mondal, J. Roy, D. Mondal, S. Bardhan, A. Majumdar and S. Das, *J. Mol. Struct.*, 2024, **1298**, 136996.

35 D. Mondal, N. Bag, J. Roy, S. Ghosh, S. Roy, M. Sarkar, S. Bardhan, S. Sutradhar and S. Das, *Langmuir*, 2024, **40**, 5785–5798.

36 C. Chen, S. Roy, J. Wang, X. Lu, S. Li, H. Yang, M. Cheng, B. Guo and Y. Xu, *Pharmaceutics*, , DOI:10.3390/pharmaceutics15082155.

37 P. Halder, I. Mondal, N. Bag, T. Hassan and S. Biswas, *Colloids Surfaces A Physicochem. Eng. Asp.*, 2025, **705**, 135546.